Catalysis Today 154 (2010) 85–91

Contents lists available at ScienceDirect

Catalysis Today

journal homepage: www.elsevier.com/locate/cattod

Selective poisoning of active sites for D_2 dissociation on platinum

Christine Hahn [a,*], Junjun Shan [a], Irene M.N. Groot [a,b], Aart W. Kleyn [a,b], Ludo B.F. Juurlink [a]

[a] Leiden Institute of Chemistry, Leiden University, P.O. Box 9502, 2300 RA Leiden, The Netherlands
[b] FOM Institute for Plasma Physics Rijnhuizen, P.O. Box 1207, 3430 Nieuwegein, The Netherlands

ARTICLE INFO

Article history:
Available online 24 February 2010

Keywords:
Single crystal
Platinum
Hydrogen
Carbon monoxide
Coadsorption
Poisoning

ABSTRACT

We have examined the reactivity of D_2 on CO-precovered Pt(5 3 3) employing supersonic molecular beam techniques and compare our results to D_2 dissociation on the bare surface. At very low kinetic energy, reaction probability is reduced linearly with increasing CO-precoverage at step edges. Diffusion of molecularly bound hydrogen along the step edge can therefore be excluded. In addition, CO adsorption at steps increases the barrier to direct dissociation at terrace sites by ~14 kJ/mol. A comparison to results from a previous study [A.T. Gee, B.E. Hayden, C. Mormiche, T.S. Nunney, Surface Science 512, 165 (2002)], shows different poisoning behaviors by CO and O that may be related to their ability to react with hydrogen.

1. Introduction

The 'active site' that catalyzes reactions at metal surfaces has been one of several foci of Ben Nieuwenhuys' research throughout his professional life. In order to investigate what such active sites consist of and how they catalyze reactions, Ben has used traditional catalytic research employing metallic particles and surface science techniques on well-defined single crystal surfaces. This combination is rather unique as most scientists opt to focus their efforts on a single type of research. Ben's contributions to the field also cover a wide range of topics, from oscillatory reactions to three-way catalytic convertors, employing techniques from high pressure catalysis with GC–MS detection down to ultra-high vacuum (UHV) conditions using scanning tunneling microscopy (STM). One of his two most recent foci is Au catalysis, where again, he used both, supported particles as well as flat and stepped single crystal surfaces [1–8].

Steps on otherwise flat single crystal surfaces are often considered to resemble active sites for dissociation of rather stable molecules. For methane activation on Ni(1 1 1), the dissociation probability is two orders of magnitude higher at step sites compared to terrace sites [9]. For N_2 activation on Ru(0 0 0 1), the difference is even in the range of nine orders of magnitude [10]. Research on the role of step sites with regards to hydrogen–deuterium exchange was initiated by Somorjai and co-workers. His group showed that step sites significantly facilitate H–D exchange on Pt(9 9 7), Pt(5 5 3), Pt(3 3 2) and Pt(7 5 5) [11–13]. In addition, they found that the reaction prefers that incident molecules impinge on the open side of the step edge [12,13].

More recent experimental [14–17] and theoretical [18,19] research on H_2 (D_2) dissociation on the active (1 0 0) step site on various Pt surfaces has deepened our knowledge of the mechanisms by which such sites induce reactivity. At low kinetic energy of impinging H_2 molecules, step sites provide an indirect mechanism to dissociation that is absent on extended flat (1 1 1) terraces. Surface corrugation converts the velocity component of impinging hydrogen molecules oriented perpendicular to the surface to a velocity component parallel to the surface. Hydrogen molecules become temporarily trapped in molecular chemisorption wells located at the bottom of the (1 0 0) steps. This molecular precursor diffuses along the longer axis of the unit cell before dissociating at the top of the active step site, where no barrier for dissociation exists (see Section 4.2 and Fig. 5 for more detailed explanation). In addition, at all kinetic energies, H_2 molecules may also react through a direct mechanism without encountering a barrier to dissociation when impinging directly onto the top of the active step site. We have recently shown that the cross-section for this process is ~3.7 Å^2 [17]. At high kinetic energy, H_2 molecules may dissociate by a direct mechanism on (1 1 1) terrace sites, which appears not significantly different from that occurring on extended (1 1 1) terraces [16–18,20].

Besides active sites required for strongly activated reactions, poisoning and promoting effects of coadsorbates are crucial to catalysis [21]. The effects of coadsorbates are not as straightforward as they might appear prima facie. For example, electropositive potassium acts as a promoter in the Born-Haber process of ammonia synthesis [22–24], but as a poison for hydrogen

* Corresponding author. Visiting address: Leiden University, LIC, Einsteinweg 55, 2333 CC Leiden, The Netherlands. Tel.: +31 715274252; fax: +31 715274451.
E-mail address: c.hahn@chem.leidenuniv.nl (C. Hahn).

0920-5861/$ – see front matter © 2010 Elsevier B.V. All rights reserved.
doi:10.1016/j.cattod.2009.12.013

dissociation on Pt(1 1 1) [25] and Ni(1 1 1) [26]. Electronegative oxygen has a coverage-dependent promoting and poisoning effect for H_2 dissociation on Ni(1 1 1) [26], whereas it primarily poisons the indirect reaction channels created by (1 0 0) step sites on the Pt(5 3 3) surface [27].

In low-temperature hydrogen fuel cell catalysis, poisoning by CO is considered a significant problem, as the fuel is preferably produced by reforming (oxygenated) hydrocarbons. Thus, the hydrogen feed tends to contain large amounts of CO [28,29]. The presence of CO in a fuel cell cannot only hamper hydrogen dissociation at the catalyst, but it can also change properties of the membrane electrode assembly, like hydrophobility and hydrophobicity or proton transportation pathways and water management [28].

In this paper, we investigate the poisoning of hydrogen dissociation by CO at the active (1 0 0) step site on platinum. We use a Pt(5 3 3) single crystal to provide these (1 0 0) step sites and investigate how CO interferes with the dissociation of D_2 as a function of CO-precoverage and D_2 kinetic energy. We compare our results to those obtained by Gee et al. [27] for the O_{step}-precovered surface. We also discuss our results with respect to a potential energy surface (PES) for H_2/Pt(2 1 1), and classical trajectory [18] and quantum dynamical calculations [19] that predict reactivity.

2. Experimental methods

Experiments were conducted using an ultra-high vacuum (UHV) apparatus equipped with a double differentially pumped supersonic molecular beam source as described elsewhere [30,31]. During experiments, the base pressure was 2×10^{-10} mbar. The platinum single crystal (5N5) was cut and polished to within 0.1° of the (5 3 3) surface (Surface Preparation Laboratory, Zaandam, The Netherlands). The surface structure of the (5 3 3) plane of a fcc metal is also described as [4(1 1 1) × (1 0 0)], i.e. a stepped surface with, on average, 4-atom wide (1 1 1) terraces separated by (1 0 0) steps. The surface was cleaned by repeated cycles of Ar^+ bombardment, annealing at 900 K in 2×10^{-8} mbar O_2 and at 1200 K without O_2 for several minutes each. In previous studies, these procedures were found to adequately clean the surface, yield the expected low-energy electron diffraction (LEED) pattern and the correct CO and NO temperature programmed desorption traces [32–36]. Our subsequent experiments on the cleaned surface involve dosing CO from the background, impinging D_2 from a supersonic molecular beam and finally performing a temperature programmed desorption (TPD) experiment as described in detail below.

Onto the clean and well-ordered surface, CO was dosed by background dosing (1.5×10^{-8} mbar, 100 s) up to saturation at T_{surf} = 300 K. Excess CO was removed by flashing and/or annealing the crystal at different temperatures for 100 s. Flashing the crystal to 420 K removes all terrace-bound CO [32]. These procedures yield in our experience the most reproducible remaining CO coverage. We have determined the maximum TPD integral for CO from a series of increasing CO exposures. Others have reported the maximum CO coverage on Pt(5 3 3) to be 0.63 CO/Pt [33]. As we cannot determine the absolute coverage of CO independently, we use "1 ML" for the saturation coverage and use it as a reference for all other reported CO coverages. We report the coverages as determined after every individual experiment. Differences between CO coverages that were or were not impinged upon by D_2 are within experimental error. For all TPD measurements, we have used the differentially pumped quadrupole mass spectrometer (Baltzers QME 421) at a fixed distance of 5 mm and normal to the Pt(5 3 3) crystal.

The CO-covered Pt(5 3 3) surface is subsequently exposed to D_2 from a supersonic molecular beam, created by expansion of mixtures of D_2 (Linde gas, isotopic purity 2.8) in Ar (Hoekloos, 6N) or H_2 (Hoekloos, 6N) and pure D_2. Expansion is performed between 2×10^3 and 4×10^3 mbar through a tungsten nozzle with a diameter of 60 μm. Two downstream skimmers create a 6 mm diameter beam impinging onto the center of the 10 mm diameter Pt single crystal. The kinetic energy of the D_2 beam was varied by changing the nozzle temperature from room temperature to 1300 K and/or seeding ratios. The kinetic energy of D_2 is determined for all beam conditions by time-of-flight (TOF) spectrometry by varying the neutral flight path length to the differentially pumped mass spectrometer. The slope of a graph plotting the flight time versus QMS position provides an accurate value of the most probable velocity. Kinetic energies reported in this paper for D_2 are calculated from this velocity.

As the reaction probability is high, minor amounts of vibrational excitation upon heating the nozzle do not affect the reaction probability significantly. The reported reaction probabilities may be taken to be that of the vibrational ground state. The rotational distribution is determined by the expansion temperature. Rotational relaxation in supersonic expansions of D_2 has been studied in detail for a large range of stagnation pressures and temperatures [37]. For the expansion conditions employed in this study up to at least 500 K, the rotational temperature of our beams is ~0.8 of the nozzle temperature. Reaction probabilities are determined using the King and Wells technique [38] with an inert flag in the main UHV chamber. All King and Wells measurements were performed using a second quadrupole mass spectrometer (Baltzers QME 125), which is located at a large distance and not in line-of-sight from the molecular beam and single crystal.

Finally, after exposing the surface to the D_2 molecular beam, a TPD experiment is performed with a heating rate of 1 K/s up to 650 K to verify the CO coverage. We have monitored mass-to-charge ratios (m/e) of 2 (H_2), 3 (HD), 4 (D_2) and 28 (CO). We do not find evidence for significant contamination by H_{ads} (<0.05 ML) during the experiment.

To obtain reproducible results, crystal cleaning by sputtering and annealing cycles was required after every single experiment that determined the reaction probability of D_2 onto CO-covered Pt(5 3 3). Failure to clean the surface after such an experiment lead immediately to significantly lowered reactivity for D_2 in the subsequent measurement, even if it was performed on the bare Pt(5 3 3) surface. We have not pursued the origin of this observation in detail.

3. Results

3.1. CO desorption

Fig. 1 presents TPD spectra of CO desorbing from the Pt(5 3 3) surface. We observe that CO desorbs in two peaks centered at 375 K and 470 K. In previous studies, the two peaks have been ascribed to desorption from terraces and steps, respectively [33–36,39]. We have fitted TPD features by a summation of horizontally shifted Gaussian functions and used their integrals to determine relative coverages. When applying the procedures described by Backus et al. [32], we find relative integrals for step and terrace desorption of 0.41:0.59.

3.2. Dependence of D_2 dissociation on CO-precoverage

Fig. 2 presents the absolute reaction probability of D_2 on Pt(5 3 3) for varying CO-precoverages. The kinetic energy of impinging D_2 was 0.8 kJ/mol. Every data point reflects the measured reactivity from a single King and Wells measurement. The solid line is the best fit to the data which includes all data points from θ_{CO} = 0 to 0.41 ML. Although the data show significant

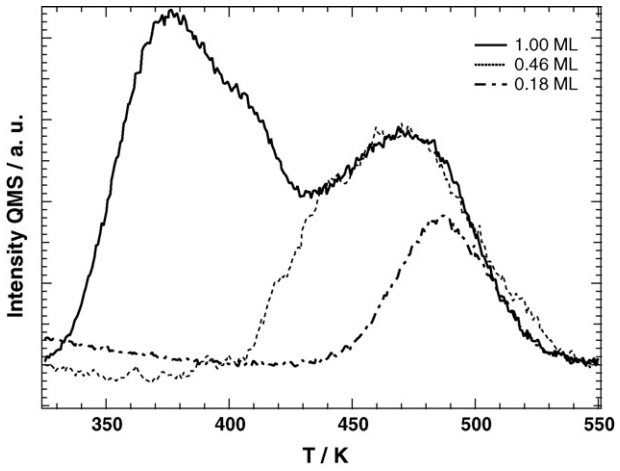

Fig. 1. Thermal desorption spectra for different dosages: full coverage (solid line), 0.46 ML (dotted line) and 0.18 ML (dash dotted line).

scatter, a linear dependence of the reaction probability on θ_{CO} seems to fit the data well and intersects the *x*-axis at 0.46 ML and the *y*-axis at 0.46. The latter is in excellent agreement with the absolute reactivity determined previously for the bare Pt(5 3 3) surface [14,27].

3.3. Hydrogen dissociation on bare Pt(5 3 3)

In Fig. 3, the reaction probability of hydrogen (both H_2 and D_2) dissociation on bare Pt(5 3 3) is shown as measured in our lab by Groot [14] (solid circles), including the best fit to our data and by Gee et al. [27] (open squares). The data are in excellent agreement, especially in the low kinetic energy regime. Every data point measured by Groot is an average of at least five single measurements. The shape of the curve has been explained in detail by theoretical studies of H_2 dissociation on the related Pt(2 1 1) surface [18]. The initial decrease in reactivity results from a precursor-mediated reaction channel that is induced by molecular chemisorption wells for D_2 at the bottom of the step–terrace border. The linear increase in reactivity at higher kinetic

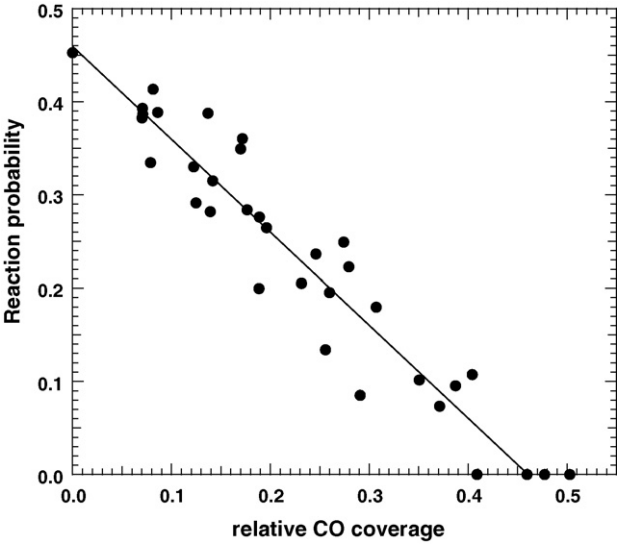

Fig. 2. Dependence of the reaction probability on CO-precoverage for the dissociation of D_2 (solid circles) on Pt(5 3 3) at a kinetic energy of 0.8 kJ/mol. The solid line is a fit for the data up to step saturation coverage of CO.

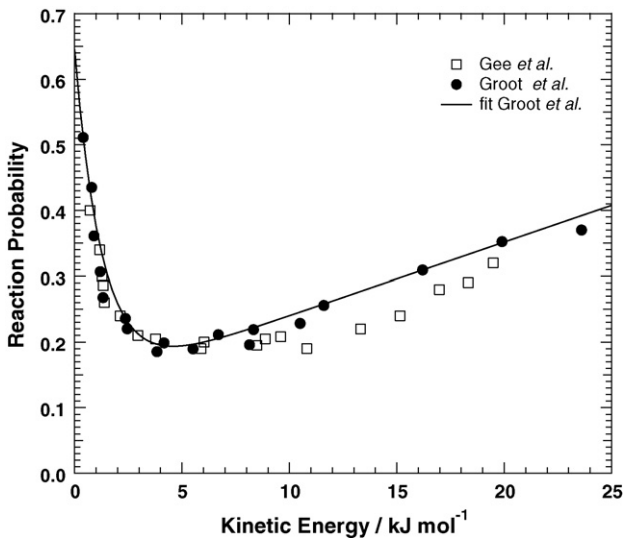

Fig. 3. Reaction probability of hydrogen dissociation on Pt(5 3 3) measured by Groot [14] (solid circles) and Gee et al. [27] (open squares). The solid line presents a fit through the data determined by Groot [14].

energies results from activated adsorption at terrace sites. When the linear part of the reactivity is extrapolated to $E_{kin} = 0$, a non-zero value for reactivity is found (namely 0.14) which is due to hydrogen molecules directly impinging onto the step where no barrier to dissociation exists [18]. As no isotope effects were observed experimentally for dissociation onto Pt(1 1 1) [20,40], Pt(2 1 1) [15], Pt(5 3 3) [14,16,27] and Pt(7 5 5) [14], we find it reasonable to discuss H_2 and D_2 dissociation without differentiating between the two isotopes.

3.4. Dependence of D_2 dissociation on kinetic energy for CO-precovered Pt(5 3 3)

Fig. 4 shows the absolute reaction probability of D_2 for a CO precoverage of 0.41 ML as a function of incident energy (solid circles). For comparison, we have included the best fit to the hydrogen reaction probability for the bare Pt(5 3 3) surface as determined in

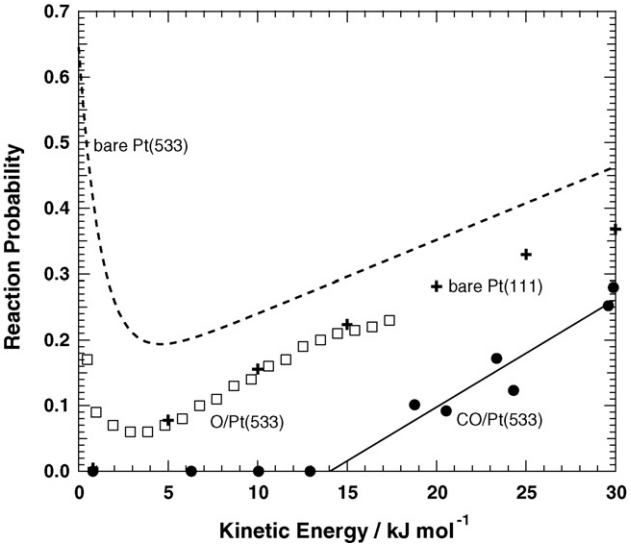

Fig. 4. Reaction probability for hydrogen–deuterium on bare [14] (dotted line), O_{step}-precovered [27] (open squares) and CO_{step}-precovered Pt(5 3 3) (solid circles) and bare Pt(111) (crosses) [20]. The solid line represents the best fit for the data points of the CO-precovered surface with measurable reactivity.

our lab (dotted line) [14] and the reaction probability on bare Pt(1 1 1) (crosses), as calculated from a fit given by Luntz et al. [20]. Fig. 4 also shows the reaction probability on the O/Pt(5 3 3) surface for step edge saturation (open squares) [27]. For D_2 dissociation on the CO-precovered surface at step edge saturation, we observe no reactivity up to E_{kin} = 13 kJ/mol. At 19 kJ/mol, we find a reactivity of ~0.1 which gradually increases with kinetic energy up to 30 kJ/mol. Assuming a linear dependence of reactivity on kinetic energy, we fit the data with measurable reactivity and find it is well described by $0.016 \times (E_{kin} - 14)$ (solid line). The energy-dependent reactivity is obviously very different from all other data shown in Fig. 4. Decorating steps by CO reduces reactivity at all energies compared to both the bare Pt(5 3 3) and Pt(1 1 1) surfaces. It also annihilates the characteristic upturn in reactivity at low kinetic energy. This is also in contrast to the reactivity of the O_{step}-precovered surface, which shows significant reactivity over the entire energy range, including the curvature change at low kinetic energy that is considered indicative of an indirect reaction mechanism.

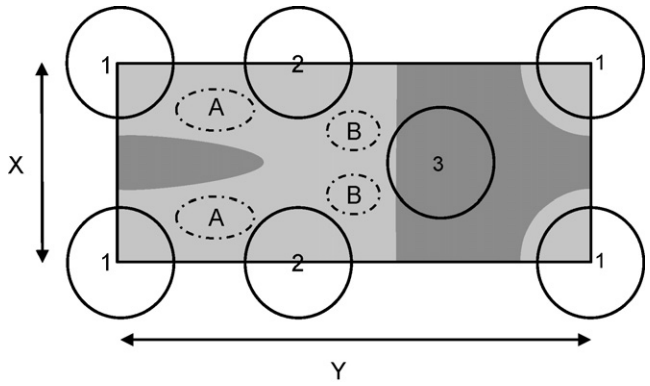

Fig. 5. Simplified representation of the potential energy surface for H_2/Pt(2 1 1) (adapted from McCormack et al. [18]).

4. Discussion

4.1. CO adsorption and desorption

Our CO TPD results shown in Fig. 1 are in general agreement with previous studies [33–36]. Most TPD studies use flash heating and find peak desorption temperatures of ~400 K and ~500 K. Our studies are performed with a heating rate of 1.0 K/s. Differences in peak temperatures therefore likely result, at least in part, from vastly differing heating rates. Tobin and co-workers reported relative integrals of 0.25:0.38 for step and terrace saturation [33,35], which equals our relative coverages of 0.41:0.59 within experimental error. Note that we use relative step and terrace coverage that sum to "1 ML", whereas Tobin and co-workers use absolute values and found the maximum CO coverage to be 0.63 CO per Pt surface atom [33,35].

As all D_2 reactivity measurements were performed at a surface temperature of 300 K, we consider the mobility of CO. As CO is generally presumed mobile at this surface temperature, the surface will be in an equilibrated state [41]. Backus et al. [32] studied the diffusion of CO on Pt(5 3 3) by ultrafast pump-probe vibrational spectroscopy and found that step-bound CO, which was excited by a laser pulse to move it to the terrace, quickly diffused back to step sites [32]. Other studies employing various techniques corroborated that CO_{step} is by far the more stable species [33,42,43]. From DFT calculations, the binding energy difference between step and terrace sites is found to be ~0.2 eV. A double peaked 0.4 eV diffusion barrier hampers movement from the top edge of the step onto the (1 1 1) plane [32]. In addition, a recent XPS study on the 1-atom wider Pt(3 2 2) surface showed that, at step saturation coverage, almost all CO was located at the step sites at 290 K [44]. Therefore, the distribution of CO bound to steps and terraces at coverages at or below step saturation is strongly in favor of step sites at 300 K. In our experiments, we assume that when D_2 molecules impinge onto a CO-precovered surface, almost all CO molecules reside at step sites up to θ_{CO} ~0.41 ML.

4.2. Mechanisms towards hydrogen dissociation

Before discussing our results for the effect of CO adsorption on the active (1 0 0) step site, we summarize some general aspects of hydrogen dissociation on stepped platinum surfaces. It has been known for some time that step sites significantly increase reactivity of metal surfaces towards isotope exchange (see for example the review by Somorjai [45]). In recent years, the most detailed understanding of the mechanisms by which hydrogen dissociates at active step sites resulted from high-dimensional, theoretical studies. For H_2/Pt(2 1 1), a surface consisting of 3-atom wide (1 1 1) terraces separated by (1 0 0) steps, McCormack et al. [18] calculated a state-of-the-art potential energy surface (PES). The contours of this PES in the *X*–*Y* plane are reproduced schematically in Fig. 5. Large solid circles indicate the platinum atoms of the unit cell. Atoms #1 and #2 are the top and bottom edge atoms in the step, respectively. Atom #3 is located approximately at the center of what is generally considered the terrace. Light grey areas represent attractive interaction between molecular hydrogen and the surface, while dark grey areas indicate repulsive interaction. Within the attractive region, molecular chemisorption wells (dash dotted lines, indicated by letters A and B) stabilize a molecular precursor. Barrier-free dissociation of H_2 occurs only at #1 step edge atoms.

The authors observe three reaction pathways in classical trajectory [18] and quantum mechanical dynamics [19] simulations of H_2 dissociation. The first mechanism is an indirect, non-activated mechanism, dominating at low kinetic energies. It involves a mobile precursor moving from wells B to A before dissociating at a Pt atom #1. The second is a direct, non-activated mechanism for molecules impinging directly onto a Pt atom #1. The third is the direct, activated channel, dominating at high kinetic energies for molecules impinging at Pt atom #3. While the two non-activated channels dominate reactivity at low kinetic energies, the contribution of the indirect pathway decreases rapidly with increasing kinetic energy. This latter dependence reflects a decreasing trapping probability in molecular chemisorption wells with increasing kinetic energy. The combination of these three mechanisms causes the characteristic energy-dependence for the absolute reactivity, which starts high, decreases initially with increasing kinetic energy before ultimately increasing again. An experimental study by Groot et al. [15] employing a Pt(2 1 1) surface and supersonic molecular beam techniques supports the findings by McCormack et al. [18] for this particular surface although the absolute values for reactivity differ slightly.

The energy dependence of reactivity on Pt(5 3 3) shown in Fig. 3 indicates that the same mechanisms also operate on the surface consisting of 1-atom longer terraces. Comparing experimental data for Pt(2 1 1) [15] and Pt(5 3 3), the relative contribution of the indirect dissociation pathway to the overall reactivity is reduced slightly. A more detailed study that investigates the influence of terrace length will be published elsewhere [17]. That study concludes that a quantitative model based on these three reaction mechanisms reproduces the observed reactivity on 3-atom wide Pt(2 1 1), 4-atom wide Pt(5 3 3) and 6-atom wide Pt(7 5 5) surfaces. The quantitative agreement between data shown in

Fig. 3 taken by two different laboratories confirms that we may also compare data for O- and CO-precovered surfaces from the same laboratories quantitatively.

For the O-precovered surface, Gee et al. [27] found that oxygen atoms bound to (1 0 0) steps result in a lowered reaction probability compared to the bare surface at all kinetic energies (see Fig. 4). They explain their results for the bare and O_{step}-precovered surface in terms of four pathways to dissociation in contrast to three found by McCormack et al. [18]. Gee et al. distinguish between an unaccommodated molecular precursor state, contributing to reactivity below ~14 kJ/mol and an accommodated molecular precursor state contributing only below ~3 kJ/mol [16,27]. Their results for the O_{step}-precovered surface are interpreted to indicate that O bound to the top of the (1 0 0) step edge blocks the channel that is active up to ~14 kJ/mol while the channel below ~3 kJ/mol remains open. This explains the change in curvature of the reactivity near 3 kJ/mol. They observe that this latter channel even stays active when the terrace is partially covered with oxygen. Direct, activated dissociation on the (1 1 1) terrace is not significantly affected by oxygen atoms bound to the step as the reactivity at high kinetic energy nearly equals that in value and slope of the Pt(1 1 1) surface.

4.3. Dependence of D_2 dissociation on CO-precoverage

We interpret our results in Fig. 2 in terms of the two relevant mechanisms as proposed by McCormack et al. for dissociation of hydrogen with low kinetic energy. At E_{kin} = 0.8 kJ/mol, an activated mechanism at the terrace may be neglected entirely and we only consider the direct and indirect mechanisms that lead to dissociation at the step edge. In previous studies [14,15,17] we have not found the surface temperature dependence observed by Gee et al. and we see no need to distinguish between different types of precursors. Fig. 2 shows that the reactivity of slow moving D_2 molecules is linearly dependent on the CO coverage at the step. The linear fit to the data indicates that at a relative CO coverage of 0.46 reactivity has dropped to zero. This value is very close to 0.41 at which step edges are saturated with CO.

First, we consider the direct mechanism. As CO is chemically bound to the step edge by approximately 2 eV, it is safe to assume that non-activated, direct dissociation of hydrogen at the same site is blocked. Previous experiments in our group investigated hydrogen dissociation on CO-precovered Ru(0 0 0 1) [46]. Here, we found that CO sterically blocks non-activated on-top dissociation with a blocking radius of ~2.5 Å. This blocking radius is independent of energy up to ~35 kJ/mol. It seems reasonable that the same steric mechanism with a similar blocking radius contributes linearly to the decrease in reactivity on the (1 0 0) active step site on Pt(5 3 3). Experiments using He atom scattering of individual CO atoms on Pt(1 1 1) also found a hard core scattering radius of 2.5 Å [47]. In Fig. 6 we present a schematic side view of CO bound to the Pt(5 3 3) surface. Here, we neglect that at high coverages, CO molecules bound to the (1 0 0) step have been reported to be tilted by ~10° from the indicated terrace normal towards the surface normal [34].

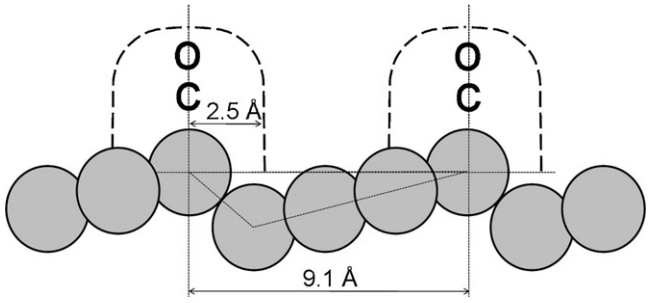

Fig. 6. A schematic side view of Pt(5 3 3) with the surface planes for the terrace, step and macroscopic surface forming a triangle and a model for steric blocking by CO (dashed lines).

To explain the linear dependence of reactivity on CO coverage up to step saturation, also the indirect contribution to reactivity must scale linearly with CO coverage. If trapped hydrogen molecules can sample multiple sites along the step edge, the reactivity dependence would be non-linear with CO coverage. In particular, from the Kisliuk model for dissociative adsorption [48] one would expect a reactivity that remains much longer close to the value found for θ_{CO} = 0 ML, especially at very low coverages. At coverages close to step edge saturation, the reaction probability would decrease steeply. As our results are in contradiction to this behavior, diffusion of a molecular hydrogen precursor along the step edge can be strictly excluded. This is also in line with results from theoretical studies of H_2 dissociation that find little diffusion along the *X*-axis of the unit cell (see Fig. 5) for molecules dissociating via a precursor mechanism on the bare Pt(2 1 1) surface [18]. The origin of that is the diffusion barrier between the deepest molecular chemisorption wells (type A in Fig. 5). In our CO_{step}/Pt(5 3 3) case, the indirect mechanism to H_2 dissociation may be affected by steric blocking of the entrance channel to molecular chemisorption, but also by electronic effects that reduce or remove the attractive wells in the D_2/Pt(5 3 3) potential.

The linear dependence of CO_{step} on D_2 dissociation presents an interesting contrast to the effect of other poisons, such as K on Pt(1 1 1) [25]. Brown, Luntz, and Shultz found large range poisoning of direct, activated D_2 dissociation by K with a cross-section, Σ_K, ranging from 70 to 430 Å^2. These values were obtained by fitting $S_0(\theta_K) = S_0 \times \exp[-n \times \theta_K]$ for various kinetic energies of D_2 and realizing that n equals the ratio of Σ_K and the unit cell area, A_{uc}; $n = \Sigma_K/A_{uc}$. When we apply the same strategy and fit $S_0(\theta_{CO}) = S_0 \times (1 - n \times \theta_{CO})$, we find Σ_{CO} = 55 Å^2. This would correspond to a blocking radius of 4.2 Å for CO, much larger than 2.5 Å found for D_2/CO/Ru(0 0 0 1) and He scattering experiments for CO on Pt(1 1 1) [47]. However, at the low kinetic energy under consideration here, there are two operative mechanisms on the Pt(5 3 3) surface which are both confined to a small area of the unit cell. Therefore, we do not consider the calculation of Σ_{CO} based on the entire area of the unit cell to yield a physically meaningful value.

4.4. Dependence of D_2 dissociation on kinetic energy for step-saturated CO

Fig. 4 shows that step-saturation by CO removes all measurable reactivity up to at least a kinetic energy of 13 kJ/mol. Clearly, the indirect mechanism and non-activated direct mechanism, requiring non-occupied Pt atoms at steps, have been poisoned effectively at θ_{CO} = 0.41. If these mechanisms were the only ones affected, the remaining direct, activated mechanism would yield reactivity at a value proportional to the fraction of the unit cell still available for this mechanism. This is the fraction of the (1 1 1) terrace that is not sterically blocked by (overhanging) CO_{step} molecules. From the schematic in Fig. 6, the accessible fraction of the (1 1 1) terrace may be expected to be significant. Similar to the case of O/Pt(5 3 3), a linear dependence on reactivity starting at the origin would be observed with a slope resembling that for H_2/Pt(1 1 1). However, our results in Fig. 4 clearly contradict this. We conclude that the direct mechanism occurring at the terrace is affected by the presence of CO at the steps. It appears that CO adsorbed at the step at step-saturation coverage induces a significant barrier to dissociation at the terrace.

The similarity between the slopes of the reaction probability's energy dependence at high kinetic energy for the CO-precovered

and bare Pt(5 3 3) surfaces provides a suggestion how the direct, activated mechanism is affected. Similar slopes are generally interpreted to indicate that the distribution of barriers for activated adsorption is comparable. The shift of the linear dependence and its intersection with the *x*-axis at 14 kJ/mol then indicate that the barrier distribution has shifted by the same 14 kJ/mol upward relative to Pt(1 1 1). Similar interpretations of shifts in barrier distributions are common in state-resolved reactivity studies (see e.g. [49]).

For Pt(1 1 1), Brown et al. suggested that the long-range poisoning effect by K toward D_2 dissociation also resulted from an increased barrier to dissociation [25]. The electropositive character of K lowers the work function, Φ, by setting up a strong dipole field at the metal-vacuum interface. This results in a more extended evanescent decay of Pt 5 s electrons into the vacuum which increases the D_2-metal distance to the location where Pauli repulsion starts dominating the interaction. As the Born-Oppenheimer approximation holds for hydrogen–platinum interaction [50] and the avoided crossing of the strongly attractive atomic D potential with the repulsive molecular D_2 potential is moved further away from the surface, an increased barrier is expected from the K-induced dipole at the surface. Poelsema et al. also found a decrease in the work function when CO adsorbs to Pt(1 1 1) steps on surfaces vicinal to Pt(1 1 1) [51], suggesting that a CO-induced dipole field causes the observed increased barrier to dissociation of hydrogen. However, other theoretical studies have previously addressed promoter and poisoning issues and argued, e.g., the importance of surface states [52].

4.5. Comparison of step-saturated O and CO poisoning of hydrogen dissociation

To compare the poisoning effects of step-bound O and CO toward hydrogen dissociation, we present a schematic of the Pt(5 3 3) surface in Fig. 7. For the schematic indication of binding of atomic oxygen and molecular CO to the steps, we have used adsorption sites as suggested by previous experimental studies [27,33,34,39,53–58]. Oxygen occupies bridge sites at the top of the step edge and CO sits atop of every step edge Pt atom. When step edges are saturated, the CO:Pt_{step} and O:Pt_{step} coverages are 1:1 and 1:2, respectively.

We note two striking differences between the energy-dependent effects of step-saturated O and CO. First, the reactivity at low kinetic energy is not completely blocked for O and an indirect reaction pathway remains operative, whereas for CO no reactivity can be detected. Gee et al. find reason in a temperature dependence of the reactivity at low kinetic energies to state that an accommodated precursor mechanism causes the reactivity below 3 kJ/mol [27]. Although in itself this may be plausible, the occupancy of Pt atoms at the steps in both situations (doubly bound O in a 1:2 ratio and singly bound CO in a 1:1 ratio) makes it difficult to see how hydrogen may dissociate at the step, even if a long-lived precursor is present. The authors do not discuss how or where H_2 reacts at low kinetic energy with O poisoning all step sites. We suggest that direct reaction of H_2 with O_{step} to form OH + H or H_2O may underlie the observed reactivity. On Pt(1 1 1), formation of OH and water from adsorbed O with impinging H_2 was already identified by Mitchell and White using high resolution electron energy loss spectroscopy [59]. The formation of water on Pt(5 3 3) was studied by Skelton et al. [60]. They monitored the formation of water from adsorbed O and H at various coverages. For the bare Pt(5 3 3) surface, they observe that when the step sites are covered by O, the reaction with H from terrace sites occurs at temperatures even below 180 K at the lowest H coverages. Multiple other reaction pathways open up at higher temperatures. Similar results were recently obtained by our group [61]. The literature provides, to the best of our knowledge, no reason to expect that step-bound CO reacts with H or H_2. This may be the cause for the discrepancy observed at low kinetic energy.

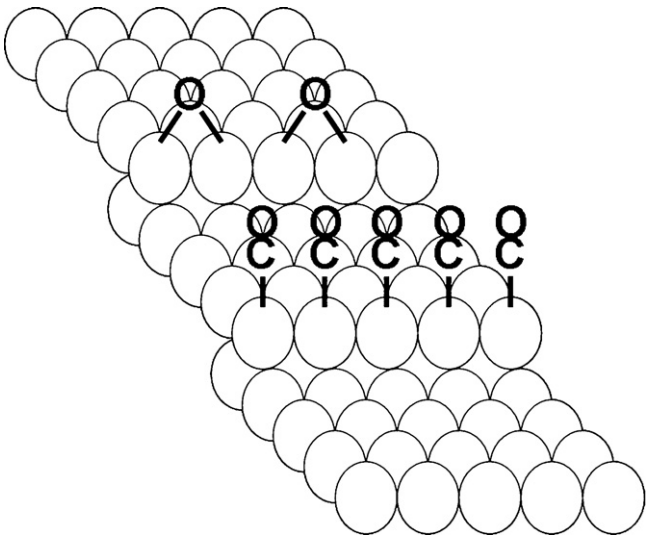

Fig. 7. Schematic of Pt(5 3 3) with adsorbed O and CO at the step edges.

The second striking difference is the variation in reactivity when direct dissociation dominates. For CO-covered steps an increased barrier to reaction is present at the terraces that appears absent for O-covered steps. As the steric blocking radius for O and CO may be expected to be comparable, a similar fraction of the terrace is accessible for molecular hydrogen. The much higher reactivity of the O-decorated surface than suggests that either oxygen has, unlike CO, little effect on the interaction between hydrogen and the Pt(1 1 1) terrace or a direct reaction path between H_2 and O provides a chemical route to reaction at all energies. As Gee et al. noticed that reactivity was also observed at low kinetic energy when more than the steps were covered by O, the latter seems an appealing option.

5. Conclusion

Preadsorption of CO at (1 0 0) step edges of Pt(5 3 3) modifies Pt's ability to dissociatively adsorb hydrogen in different ways. First, both direct and indirect pathways for D_2 dissociation at low kinetic energies are poisoned. The observed linear dependence of reactivity on step edge CO-coverage indicates that diffusion of molecularly bound hydrogen along the step edge does not occur. Second, step-bound CO induces a significant barrier for direct, activated reaction at the terrace. By analogy to the effect of potassium, we suggest that this may be the result of the strong dipole field created by CO that affects the location where Pauli repulsion becomes dominant for H_2/Pt. Finally, from a comparison of the poisoning effects toward hydrogen dissociation by O and CO bound to the active (1 0 0) step, we conclude that these poisons show different behaviors which may, at least in part, be caused by their differing ability to react with H and/or H_2.

Acknowledgements

This research was financially supported by The Netherlands Organisation for Scientific Research (NWO) through the research programs Excellent Chemical Research (ECHO) and Advanced Sustainable Processes by Engaging Catalytic Technologies (ASPECT) of Advanced Chemical Technologies for Sustainability (ACTS). The authors kindly acknowledge the Foundation for Fundamental Research on Matter (FOM) for use of equipment.

References

[1] C.J. Weststrate, E. Lundgren, J.N. Andersen, E.D.L. Rienks, A.C. Gluhoi, J.W. Bakker, I.M.N. Groot, B.E. Nieuwenhuys, Surface Science 603 (2009) 2152.
[2] A. Hussain, D. Curulla Ferré, J. Gracia, B.E. Nieuwenhuys, J.W. Niemantsverdriet, Surface Science 603 (2009) 2734.
[3] A. Georgaka, D. Gavril, V. Loukopoulos, G. Karaiskakis, B.E. Nieuwenhuys, Journal of Chromatography A 1205 (2008) 128.
[4] M.J. Lippits, R.R.H. Boer Iwema, B.E. Nieuwenhuys, Catalysis Today 145 (2009) 27.
[5] N. Aldea, V. Rednic, S. Pintea, P. Marginean, B. Barz, A. Gluhoi, B.E. Nieuwenhuys, M. Neumann, X. Yaning, F. Matei, Superlattices and Microstructures 46 (2009) 141.
[6] U. Dahlborg, C.M. Bao, M. Calvo-Dahlborg, F. Devred, B.E. Nieuwenhuys, Journal of Materials Science 44 (2009) 4653.
[7] F. Devred, A.H. Gieske, N. Adkins, U. Dahlborg, C.M. Bao, M. Calvo-Dahlborg, J.W. Bakker, B.E. Nieuwenhuys, Applied Catalysis A: General 356 (2009) 154.
[8] M.J. Lippits, A.C. Gluhoi, B.E. Nieuwenhuys, Catalysis Today 137 (2008) 446.
[9] F. Abild-Pedersen, O. Lytken, J. Engbæk, G. Nielsen, I. Chorkendorff, J.K. Nørskov, Surface Science 590 (2005) 127.
[10] S. Dahl, A. Logadottir, R.C. Egeberg, J.H. Larsen, I. Chorkendorff, E. Törnqvist, J.K. Nørskov, Physical Review Letters 83 (1999) 1814.
[11] S.L. Bernasek, G.A. Somorjai, The Journal of Chemical Physics 62 (1975) 3149.
[12] M. Salmeron, R.J. Gale, G.A. Somorjai, The Journal of Chemical Physics 67 (1977) 5324.
[13] T.H. Lin, G.A. Somorjai, The Journal of Chemical Physics 81 (1984) 704.
[14] I.M.N. Groot, The Fight for a Reactive Site, Leiden University, 2009.
[15] I.M.N. Groot, K.J.P. Schouten, A.W. Kleyn, L.B.F. Juurlink, The Journal of Chemical Physics 129 (2008) 224707.
[16] A.T. Gee, B.E. Hayden, C. Mormiche, T.S. Nunney, The Journal of Chemical Physics 112 (2000) 7660.
[17] I.M.N. Groot, K.J.P. Schouten, A.W. Kleyn, L.B.F. Juurlink, submitted for publication.
[18] D.A. McCormack, R.A. Olsen, E.J. Baerends, The Journal of Chemical Physics 122 (2005) 194708.
[19] R.A. Olsen, D.A. McCormack, M. Luppi, E.J. Baerends, The Journal of Chemical Physics 128 (2008) 194715.
[20] A.C. Luntz, J.K. Brown, M.D. Williams, The Journal of Chemical Physics 93 (1990) 5240.
[21] G.A. Somorjai, Introduction to Surface Chemistry and Catalysis, John Wiley & Sons, Inc, New York, 1994.
[22] P. Moggi, G. Albanesi, G. Predieri, G. Spoto, Applied Catalysis A: General 123 (1995) 145.
[23] A. Ozaki, K.-i. Aika, H. Hori, Bulletin of the Chemical Society of Japan 44 (1971) 3216.
[24] G. Ertl, S.B. Lee, M. Weiss, Surface Science 114 (1982) 527.
[25] J.K. Brown, A.C. Luntz, P.A. Schultz, The Journal of Chemical Physics 95 (1991) 3767.
[26] C. Resch, V. Zhukov, A. Lugstein, H.F. Berger, A. Winkler, K.D. Rendulic, Chemical Physics 177 (1993) 421.
[27] A.T. Gee, B.E. Hayden, C. Mormiche, T.S. Nunney, Surface Science 512 (2002) 165.
[28] X. Cheng, Z. Shi, N. Glass, L. Zhang, J. Zhang, D. Song, Z.S. Liu, H. Wang, J. Shen, Journal of Power Sources 165 (2007) 739.
[29] R.J. Behm, Z. Jusys, Journal of Power Sources 154 (2006) 327.
[30] H.G. Jenniskens, A. Bot, P.W.F. Dorlandt, W. van Essenberg, E. de Haas, A.W. Kleyn, Measurement Science and Technology 8 (1997) 1313.
[31] B. Riedmüller, F. Giskes, D. Glastra van Loon, P. Lassing, A.W. Kleyn, Measurement Science and Technology 13 (2002) 141.
[32] E.H.G. Backus, A. Eichler, A.W. Kleyn, M. Bonn, Science 310 (2005) 1790.
[33] J.S. Luo, R.G. Tobin, D.K. Lambert, G.B. Fisher, C.L. DiMaggio, Surface Science 274 (1992) 53.
[34] J.S. Somers, T. Lindner, M. Surman, A.M. Bradshaw, G.P. Williams, C.F. McConville, D.P. Woodruff, Surface Science 183 (1987) 576.
[35] H. Wang, R.G. Tobin, D.K. Lambert, The Journal of Chemical Physics 101 (1994) 4277.
[36] J. Xu, J.T. Yates, Surface Science 327 (1995) 193.
[37] K. Kern, R. David, G. Comsa, The Journal of Chemical Physics 82 (1985) 5673.
[38] M.G. Wells, D.A. King, Proceedings of the Royal Society of London Series A: Mathematical Physical and Engineering Sciences 339 (1974) 245.
[39] B.E. Hayden, K. Kretzschmar, A.M. Bradshaw, R.G. Greenler, Surface Science 149 (1985) 394.
[40] P. Samson, A. Nesbitt, B.E. Koel, A. Hodgson, The Journal of Chemical Physics 109 (1998) 3255.
[41] H.R. Siddiqui, X. Guo, I. Chorkendorff, J.T. Yates Jr, Surface Science 191 (1987) L813.
[42] J.E. Reutt-Robey, D.J. Doren, Y.J. Chabal, S.B. Christman, Physical Review Letters 61 (1988) 2778.
[43] J. Ma, X. Xiao, N.J. DiNardo, M.M.T. Loy, Physical Review B 58 (1998) 4977.
[44] B. Tränkenschuh, C. Papp, T. Fuhrmann, R. Denecke, H.P. Steinrück, Surface Science 601 (2007) 1108.
[45] G.A. Somorjai, The Journal of Physical Chemistry B 106 (2002) 9201.
[46] H. Ueta, I.M.N. Groot, M.A. Gleeson, S. Stolte, G.C. McBane, L.B.F. Juurlink, A.W. Kleyn, Chemphyschem 9 (2008) 2372.
[47] A.M. Lahee, J.R. Manson, J.P. Toennies, C. Wöll, The Journal of Chemical Physics 86 (1987) 7194.
[48] P. Kisliuk, Journal of Physics and Chemistry of Solids 5 (1958) 78.
[49] L.B.F. Juurlink, D.R. Killelea, A.L. Utz, Progress in Surface Science 84 (2009) 69.
[50] P. Nieto, E. Pijper, D. Barredo, G. Laurent, R.A. Olsen, E.J. Baerends, G.J. Kroes, D. Farias, Science 312 (2006) 86.
[51] B. Poelsema, R.L. Palmer, G. Comsa, Surface Science 123 (1982) 152.
[52] E. Bertel, N. Memmel, Applied Physics A: Materials Science & Processing 63 (1996) 523.
[53] H. Wang, R.G. Tobin, D.K. Lambert, C.L. DiMaggio, G.B. Fisher, Surface Science 372 (1997) 267.
[54] P.J. Feibelman, J. Hafner, G. Kresse, Physical Review B 58 (1998) 2179.
[55] A.T. Gee, B.E. Hayden, The Journal of Chemical Physics 113 (2000) 10333.
[56] P.J. Feibelman, S. Esch, T. Michely, Physical Review Letters 77 (1996) 2257.
[57] Z. Sljivancanin, B. Hammer, Surface Science 515 (2002) 235.
[58] P. Gambardella, Z. Sljivancanin, B. Hammer, M. Blanc, K. Kuhnke, K. Kern, Physical Review Letters 87 (2001) 056103.
[59] G.E. Mitchell, J.M. White, Chemical Physics Letters 135 (1987) 84.
[60] D.C. Skelton, R.G. Tobin, G.B. Fisher, D.K. Lambert, C.L. DiMaggio, The Journal of Physical Chemistry B 104 (1999) 548.
[61] M.J.T.C. van der Niet, O.T. Berg, L.B.F. Juurlink, M.T.M. Koper, in preparation.